arXiv:1610.05880v2 [cond-mat.str-el] 5 Nov 2016

Doping Effects on the Electronic Structure of an Anisotropic Kondo Semiconductor $CeOs_2Al_{10}$: An Optical Study with Re and Ir Substitution

Shin-ichi Kimura[1,2*], Hitoshi Takao[2], Jo Kawabata[3], Yoshihiro Yamada[3], and Toshiro Takabatake[3,4]

[1]*Graduate School of Frontier Biosciences, Osaka University, Suita, Osaka 565-0871, Japan*
[2]*Department of Physics, Osaka University, Toyonaka, Osaka 560-0043, Japan*
[3]*Department of Quantum Matter, ADSM, Hiroshima University, Higashi-Hiroshima, Hiroshima 739-8530, Japan*
[4]*Institute for Advanced Materials Research, Hiroshima University, Higashi-Hiroshima, Hiroshima 739-8530, Japan*

(Received October 19, 2016, Accepted November 2, 2016)

An anisotropic Kondo semiconductor $CeOs_2Al_{10}$ exhibits an unusual antiferromagnetic order at rather high transition temperature T_0 of 28.5 K. Two possible origins of the magnetic order have been proposed so far, one is the Kondo coupling of the hybridization between the conduction (c) and the $4f$ states and the other is the charge-density wave/charge ordering along the orthorhombic b axis. To clarify the origin of the magnetic order, we have investigated the electronic structure of hole- and electron-doped $CeOs_2Al_{10}$ [$Ce(Os_{1-y}Re_y)_2Al_{10}$ and $Ce(Os_{1-x}Ir_x)_2Al_{10}$, respectively] by using optical conductivity spectra along the b axis. The intensity of the c-f hybridization gap at $\hbar\omega \sim 50$ meV continuously decreases from $y = 0.10$ to $x = 0.12$ via $x = y = 0$. The intensity of the charge excitation observed at $\hbar\omega \sim 20$ meV has the maximum at $x = y = 0$ as similar with the doping dependence of T_0. The fact that the charge excitation is strongly related to the magnetic order strengthens the possibility of the charge density wave/charge ordering as the origin of the magnetic order.

Recently, materials lacking local inversion symmetry with strong spin-orbit coupling are attracting attention because of their various physical properties, such as superconductivity with a very high critical magnetic field[1] and extreme-high spin polarization of surface/bulk Rashba states.[2] The title compound, $CeOs_2Al_{10}$, can be regarded as one of materials with lacking local inversion symmetry.

The compounds CeM_2Al_{10} (M = Os and Ru) are Kondo semiconductors (KS's) with a small energy gap at low temperature.[3] The crystal structure is orthorhombic $YbFe_2Al_{10}$-type,[4] in which the Ce-M bonding forms a zigzag plane in the ac plane,[5] although so called Kondo insulators (KIs) such as SmB_6 and YbB_{12} have cubic crystal structure.[6] In the compounds with M = Os and Ru, an antiferromagnetic order appears at the temperature of about 28 K that is lower than the Kondo temperature of about 60 K.[7] The ordering temperature is much higher than that expected by the de Gennes factor.[8] The origin of the high ordering temperature has not been clarified yet. One possible origin is considered to be the low crystal symmetry and/or the lacking of local inversion symmetry.

To clarify the novel physical properties of CeM_2Al_{10}s, we have investigated the electronic structure by measuring polarized optical conductivity [$\sigma(\omega)$] spectra.[5,9,10] So far, we have revealed the anisotropic electronic structure and the anisotropic hybridization intensity between conduction (c) and $4f$ states (c-f hybridization), i.e., strong (weak) c-f hybridization in the ac plane (along the b axis). Especially, we could find that the c-f hybridization gap ($\Delta_{c\text{-}f}$) with the size of about 50 meV appears along all axes. In addition to this, we have found that a charge gap (Δ_0) with the size of 20 meV appears only along the b axis.[5,9] Since the $\Delta_F 0$ does not appear in non-magnetic $CeFe_2Al_{10}$ and is formed above T_0 in $CeOs_2Al_{10}$ (38 K) and $CeRu_2Al_{10}$ (30 K), the presence of Δ_0 seems to be related to the magnetic order, i.e., the electronic structure along the b axis plays an important role for the magnetic order.

The relation between the c-f hybridization gap and the magnetic order in $CeRu_2Al_{10}$ has been investigated by using the Rh-substituted materials [$Ce(Ru_{1-x}Rh_x)_2Al_{10}$].[11] The paper claimed that the intensity of $\Delta_{c\text{-}f}$ is strongly suppressed in between $x = 0.03$ and 0.05, suggesting that the c-f hybridization intensity drastically decreases. This result is consistent with the other results that the $4f$ electron is well localized and the c-f hybridization strength becomes weak by the 5 % substitution of Rh for Ru ($x = 0.05$).[12–14] On the other hand, with increasing x, T_0 monotonically decreases from

*E-mail address: kimura@fbs.osaka-u.ac.jp

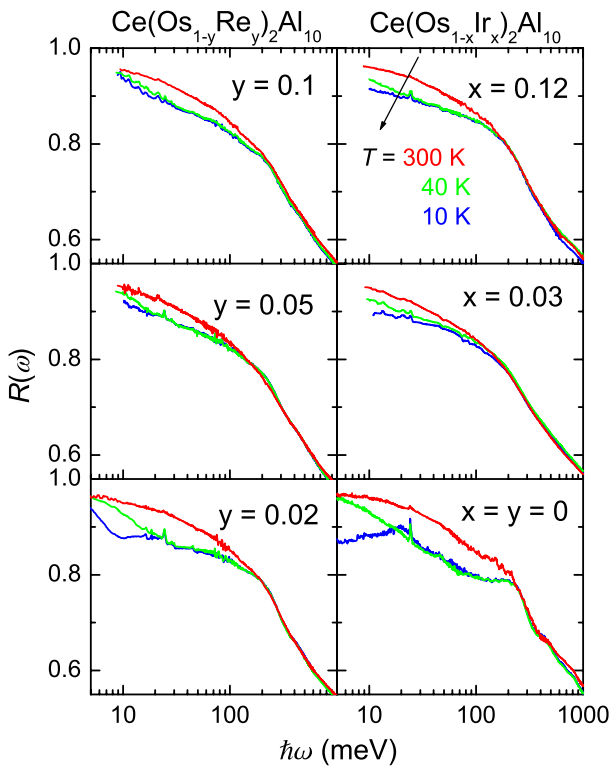

Fig. 1. (Color online) Temperature-dependent reflectivity $[R(\omega)]$ spectra of $Ce(Os_{1-y}Re_y)_2Al_{10}$ $(y = 0.02, 0.05, 0.1)$ and $Ce(Os_{1-x}Ir_x)_2Al_{10}$ $(x = 0.03, 0.12)$ along the b axis. The $R(\omega)$ spectra of $x = y = 0$ are referred from Ref. 9.

27.3 K to 24 K for $x = 0.05$ and disappears at $x \sim 0.3$.[15] The intensity of Δ_0 hardly decreases and still remains at $x = 0.05$.[11] This change in the intensity of Δ_0 is in parallel with that of T_0. However, since not only T_0 but also both of the c-f hybridization intensity and the carrier density monotonically change with x, the origin of the magnetic order cannot be concluded to be the appearance of Δ_0. In addition, the recent tunneling spectroscopic study of 5d-electron doped $CeOs_2Al_{10}$ claimed that the appearance of the magnetic order needs the c-f hybridization gap.[16,17]

In this Letter, we report the relation among T_0, Δ_0, $\Delta_{c\text{-}f}$, and the carrier density in the wide substitution range from the hole-doped $[Ce(Os_{1-y}Re_y)_2Al_{10}]$ to the electron-doped $[Ce(Os_{1-x}Ir_x)_2Al_{10}]$ materials[18] by using the $\sigma(\omega)$ spectra. As a result, the c-f hybridization intensity gradually decreases with decreasing y and increasing x, while the intensity of Δ_0 also takes maximum at $x = y = 0$ and decreases with increasing x and y. This dependence of Δ_0 is roughly in parallel to that of T_0. On the other hand, the carrier density behaves in the opposite to Δ_0. Therefore, the magnetic order is strongly related to Δ_0 and the carrier density.

Single-crystalline samples of $[Ce(Os_{1-y}Re_y)_2Al_{10}$, $y = 0.02, 0.05, 0.10$, $Ce(Os_{1-x}Ir_x)_2Al_{10}$, $x = 0.03, 0.12]$ were synthesized by the Al-flux method.[19] The composition was determined by the wavelength dispersion electron-probe microanalysis.[16] The surfaces were well-polished using 0.3 μm grain-size Al_2O_3 lapping film sheets for the optical reflectivity $[R(\omega)]$ measurements. Near-normal incident polarized $R(\omega)$ spectra were acquired in a very wide photon-energy range of 2 meV – 30 eV to ensure an accurate Kramers-Kronig analysis (KKA).[20] Martin-Puplett and Michelson type rapid-scan Fourier spectrometers (JASCO Co. Ltd., FARIS-1 and FTIR6100) were used at the photon energy $\hbar\omega$ regions of 2 – 30 meV and 5 meV – 1.5 eV, respectively, with a feed-back positioning system to maintain the overall uncertainty level less than ± 0.5 % in the temperature range of 10 – 300 K.[21] Samples were mounted in a high-vacuum cryostat ($\leq 10^6$ Pa) that includes in-situ evaporation system to cover sample with a reference gold film.

The obtained polarized $R(\omega)$ spectra of all samples in the photon energy range of 5 meV – 1 eV are plotted in Fig. 1 with those of $CeOs_2Al_{10}$ $(x = y = 0)$ referred from Ref. 9. At $T = 300$ K, $R(\omega)$ of $CeOs_2Al_{10}$ was only measured for energies 1.2–30 eV by using synchrotron radiation (not shown here), and connected to all spectra for the KKA. In order to obtain $\sigma(\omega)$ via KKA of $R(\omega)$, the spectra were extrapolated below 2 meV with a Hagen-Rubens function, and above 30 eV with a free-electron approximation $R(\omega) \propto \omega^{-4}$.[22]

The $\sigma(\omega)$ spectra for $\hbar\omega \leq 300$ meV are shown in Fig. 2(a). The wide-range $R(\omega)$ spectrum in Fig. 1 as well as the $\sigma(\omega)$ spectrum hardly changes on cooling in the photon energy range of $\hbar\omega > 300$ meV. Therefore the $\sigma(\omega)$ spectrum has temperature dependence only in the range of $\hbar\omega \leq 300$ meV. A broad peak observed at about 170 meV (mid-IR peak) in $x = y = 0$ originates from the optical transition from the valence band to the unoccupied Ce $4f_{5/2}$ state.[23] Both the peak intensity and the temperature dependence, which denote the c-f hybridization character, imply that the c-f hybridization intensity decreases with increasing x and y.[24] To clarify the temperature dependence, the center of gravity $(\langle\hbar\omega\rangle)$ below 300 meV is plotted in Fig. 2(b). The temperature dependence of $\langle\hbar\omega\rangle$ for $x = y = 0$ is the largest even though that at room temperature is comparable with those of doped samples. The temperature dependence is strongly suppressed by doping of holes and electrons, indicating the rapid collapse of the c-f hybridization band structure. Therefore we point out that this system is described by the Kondo lattice model rather than the single-site Kondo coupling model.

To compare the $\langle\hbar\omega\rangle$ of $CeOs_2Al_{10}$ with that of $CeFe_2Al_{10}$, $\langle\hbar\omega\rangle$ of $CeFe_2Al_{10}$ has been calculated using the data in Ref. 10 and plotted in Fig. 2(b). The temperature dependence of $\langle\hbar\omega\rangle$ for $x = y = 0$ is similar to that of $CeFe_2Al_{10}$ but slightly shift to the lower temperature side. Since the $\langle\hbar\omega\rangle$ indicates the temperature dependence of the Kondo coupling intensity,[25] this is quali-

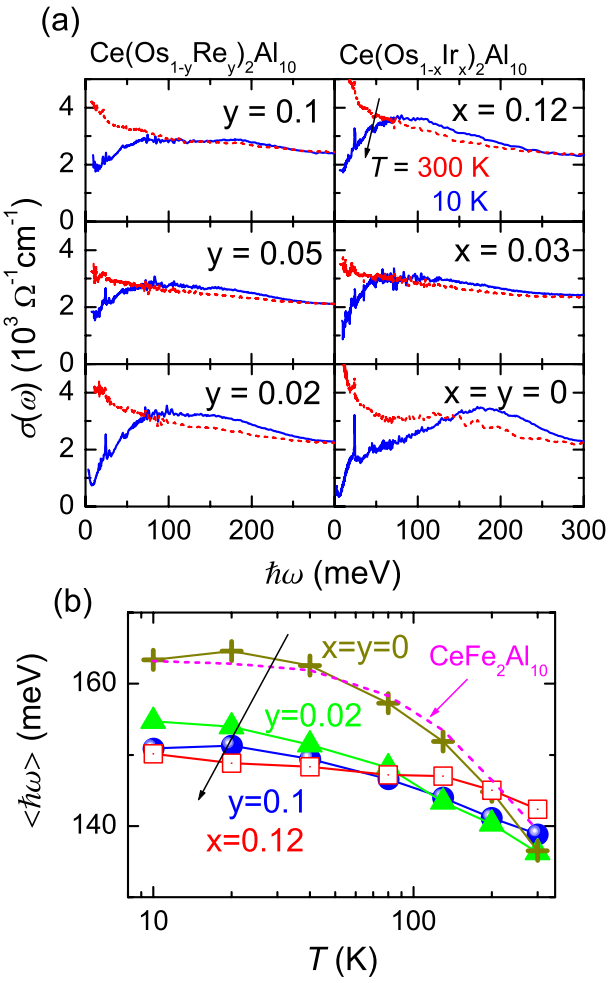

Fig. 2. (Color online) (a) Temperature-dependent optical conductivity $[\sigma(\omega)]$ spectra of $Ce(Os_{1-y}Re_y)_2Al_{10}$ ($y = 0.1, 0.05, 0.02$), $Ce(Os_{1-x}Ir_x)_2Al_{10}$ ($x = 0.12, 0.03$), and $x = y = 0$ along the b axis in the photon energy $\hbar\omega$ region below 300 meV. (b) The centers of gravity $[\langle\hbar\omega\rangle]$ of the $\sigma(\omega)$ spectra in $\hbar\omega \leq 300$ meV of $x = 0.02$ (solid triangle), 0.1 (solid circle), $x = 0.12$ (open square), $x = y = 0$ (cross), and $CeFe_2Al_{10}$ (dashed line)[10] are plotted as a function of temperature T. The error of $\langle\hbar\omega\rangle$ is less than the size of marks.

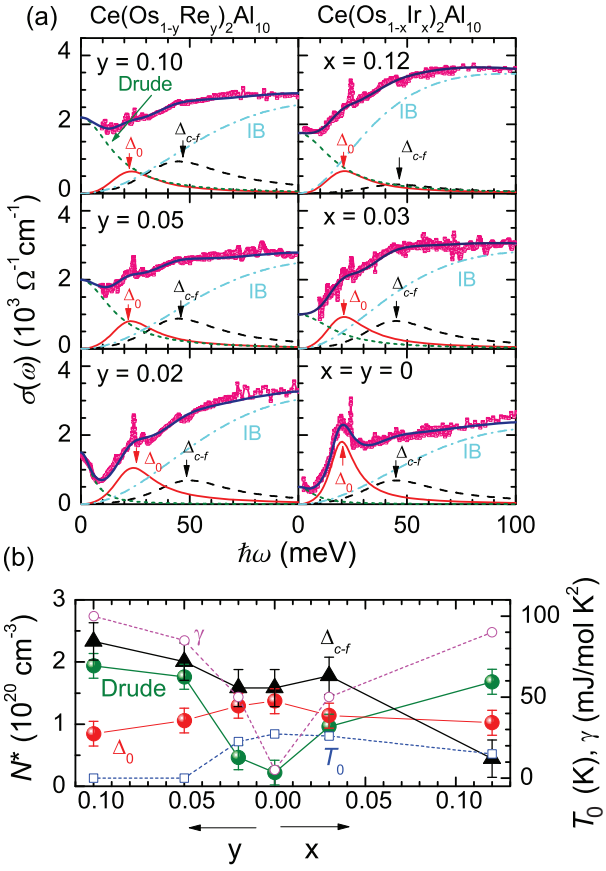

Fig. 3. (Color online) (a) $\sigma(\omega)$ spectra along the b axis at $T = 10$ K and the fitted lines of one Drude and three Lorentz functions. The three Lorentz functions are assumed as a peak (Δ_0, solid line) appearing below the magnetic ordering temperature T_0, the interband transition in the c-f hybridization gap ($\Delta_{c\text{-}f}$, dashed line), and higher interband transition from lower energy side (IB, dot-dashed line). (b) Obtained effective electron numbers (N^*s) of the Drude, Δ_0, and $\Delta_{c\text{-}f}$ components, which are plotted together with T_0 and the electronic specific heat coefficient γ as functions of the Re (y) and Ir (x) concentrations.[18]

tatively consistent with that the Kondo temperature of $CeOs_2Al_{10}$ ($\sim$ 60 K) is lower than that of $CeFe_2Al_{10}$ ($\sim$ 80 K).[7,26]

Next, we focus on the energy gap structure in the electronic structure near the Fermi level (E_F). The $\sigma(\omega)$ spectra along the b axis at $T = 10$ K in $\hbar\omega \leq 100$ meV are shown in Fig. 3(a). In this region, it should be noted that a very sharp peak owing to a transverse optical phonon is observed at around 25 meV in all samples. The temperature and concentration dependences of the peak will be discussed in a separated paper because the peak is not directly related to the electronic structure.

To clarify the change of the spectra by increasing x and y, we adopt the Drude-Lorentz fitting method that has been useful in analyzing the data for $Ce(Ru_{1-x}Rh_x)_2Al_{10}$.[11] The $\sigma(\omega)$ spectra are fitted by using the combination of Lorentz functions:

$$\sigma(\omega) = \sum_i \frac{N_i^* e^2 \tau_i \omega^2}{m_e[(\omega_i^2 - \omega^2)^2 \tau_i^2 + \omega^2]}.$$

Here, i has four components, Drude ($i = D$) with $\omega_D = 0$, Δ_0 (0), $\Delta_{c\text{-}f}$ (c-f), and a higher interband transition (IB). m_e denotes the electron rest mass. N_i^*, τ_i, and ω_i are the effective electron number, the relaxation times, and the resonant frequency of the Lorentz absorption of each component, respectively. The fitting was performed by using a least square method with keeping the peak center energies of $\hbar\omega_0$ and $\hbar\omega_{c\text{-}f}$ at 20–23 meV and 45–48 meV, respectively. Here, we assumed that the gap energies and shapes are reasonably constant against doping. The IB curves were fitted to reproduce the slope at

$\hbar\omega = 100$–120 meV. The obtained values of the effective electron number N_i^* together with T_0 and γ are plotted in Fig. 3(b) as functions of Re (y) and Ir (x) concentrations.[18]

In Figure 3(a), the Δ_0 peak of $x = y = 0$ is narrower than those of others. The reason is not clear but the corresponding peak in a tunneling spectrum is also narrower than those of doped materials.[17] Therefore, the peak shape might be reasonable and the origin should be clarified in future.

From Figure 3(b), we can get useful informations as follows:

Firstly, the doping dependence of N^*s of the Drude component (N_D^*) is qualitatively consistent with that of γ value. This is reasonable because both of the N_D^* and the γ value are proportional to the density of states at E_F. However we can recognize that the N_D^* at $y = 0.02$ is much smaller than that expected from the γ value in comparison with other concentrations. The deviation of the N_D^* from the γ value at $y = 0.02$ might originate from the mass enhancement owing to the strong electron correlation at low carrier density because $N_D^* = Nm_e/m^*$, where N and m^* are the carrier density and the effective mass of carriers, respectively, and N must be proportional to the γ value.

Secondly, the N^* of $\Delta_{c\text{-}f}$ gradually decreases with decreasing y and increasing x within error bars. This is consistent with the doping dependence of magnetic susceptibility,[18] i.e., the $4f$ state is more localized (the c-f hybridization strength decreases) with increasing electron carriers. This result is also consistent with the results obtained for the Rh doping in $CeRu_2Al_{10}$.[11] However, the doping-dependent behavior of the c-f hybridization gap is inconsistent with the behavior of the mid-IR peak shown in Fig. 2. The reason is not clear at present, but two reasons as follows are proposed: One is that the effective probing area of the c-f hybridization at the mid-IR peak might be different from that near E_F, i.e., the periodicity of the c-f hybridization can be probed by the mid-IR peaks in contrast that the average of the c-f hybridization intensity appears in $\Delta_{c\text{-}f}$ because the photon energy as well as the wavelength is much different. The other is the screening effect by carriers, i.e., the mid-IR peak is more sensitive to the carrier density than $\Delta_{c\text{-}f}$.

Lastly, the doping dependence of the N^* of Δ_0 (N_0^*) is qualitatively consistent with that of T_0. Therefore we can confirm the previous argument that the electronic structure producing the Δ_0 peak is strongly related to the magnetic order at T_0. In addition, since the N_0^* at $y = 0.05$ and 0.1 is not zero, the presence of Δ_0 is not sufficient for the magnetic order. In $CeOs_2Al_{10}$ as well as $CeRu_2Al_{10}$, Δ_0 starts to appear at slightly higher temperature (T^*) than T_0.[5,9] At temperatures between T^* and T_0, no magnetic ordering appears. The same situation might appear in $y = 0.05$ and 0.1. From the figure, we can recognize that the N_D^* has an opposite behavior to the N_0^*. This suggests that the appearance of the Δ_0 is related to the carrier density, i.e., the electronic structure of Δ_0 appears when the carrier density decreases by the gap opening owing to the strong c-f hybridization of KS. This behavior is similar to that of charge-density wave (CDW) materials[27] as well as the charge ordering (CO) material Yb_4As_3.[28]

In KIs as well as KS's, the appearance of a CDW as well as a CO phase was theoretically expected by using the periodic Anderson model with the electron correlation between carriers and $4f$ electrons, $U_{c\text{-}f}$, of proposed by Yoshida and coworkers.[29,30] In CeM_2Al_{10} (M = Os, Ru), the Δ_0 starts to open at slightly higher temperature than T_0,[9,10] which can be explained by their calculation.[29] According to the theory, the CDW/CO phase appears in the high $U_{c\text{-}f}$ region apart from the antiferromagnetic phase. The RKKY interaction as well as a magnetic order temperature is enhanced by increasing the c-f hybridization intensity owing to the renormalization effect of the $U_{c\text{-}f}$.[30] Therefore the magnetic order might occur at rather high temperatures in the presence of the CDW/CO phase.

However, in general, the effect of $U_{c\text{-}f}$ as well as the CDW/CO phase does not appear in three-dimensional KIs such as SmB_6 and YbB_{12}, but only appear in a low carrier system, Yb_4As_3.[31] The crystal structure of the latter can be regarded as composed of one-dimensional Yb chains along the $\langle 111 \rangle$ axis.[32] The CO peak of Yb_4As_3, which appears below slightly higher temperature than CO,[33] shows the similar temperature dependence to that of the N_0^* of CeM_2Al_{10}. Therefore the effect of $U_{c\text{-}f}$ is regarded to appear also in CeM_2Al_{10}. Because of no magnetic order in Yb_4As_3, however, the high-temperature magnetic order in CeM_2Al_{10} is considered to be a novel physical phenomenon owing to the $U_{c\text{-}f}$ and the anisotropic crystal structure.

In conclusion, the $5d$ hole and electron doping effects on the electronic structure of $Ce(Os_{1-y}Re_y)_2Al_{10}$ ($y = 0.02, 0.05, 0.1$) and $Ce(Os_{1-x}Ir_x)_2Al_{10}$ ($x = 0.03, 0.12$) have been investigated by using optical conductivity spectroscopy. The absorption intensity of the charge gap at $\hbar\omega \sim 20$ meV changes roughly proportional to T_0 in spite that the absorption intensity of the c-f hybridization gap at $\hbar\omega \sim 50$ meV monotonically decreases with increasing the electron dope level. The evaluated effective electron number of the Drude component is inversely proportional to the absorption intensity of the charge gap. These results suggest that the charge gap as well as the magnetic order appear at the low carrier density owing to the weak screening effect of carriers. For better understanding the obtained phenomena, theoretical studies with the periodic Anderson model with the correlation between carriers and $4f$ electrons are highly anticipated.

Acknowledgments

We would like to acknowledge H. Tanida, M. Sera, Y. Muro, A. Kondo, and T. Yoshida for their fruitful discussion and H. Yokoyama and S. Kamei for their support during optical experiments. We also thank UVSOR staff members for their technical support. Part of this work was performed under the Use-of-UVSOR Facility Program (BL1B, 2014-2016) of the Institute for Molecular Science. This work was partly supported by JSPS KAKENHI (Grant Nos. 26400363 and 16H01076).

1) E. Bauer, G. Hilscher, H. Michor, Ch. Paul, E. W. Scheidt, A. Gribanov, Yu. Seropegin, H. Noël, M. Sigrist, and P. Rogl, Phys. Rev. Lett. **92**, 027003 (2004).
2) K. Ishizaka, M. S. Bahramy, H. Murakawa, M. Sakano, T. Shimojima, T. Sonobe, K. Koizumi, S. Shin, H. Miyahara, A. Kimura, K. Miyamoto, T. Okuda, H. Namatame, M. Taniguchi, R. Arita, N. Nagaosa, K. Kobayashi, Y. Murakami, R. Kumai, Y. Kaneko, Y. Onose, and Y. Tokura, Nat. Mater. **10**, 521 (2011).
3) A. M. Strydom, Physica B **404**, 2981 (2009).
4) V. M. T. Thiede, T. Ebel, and W. Jeitschko, J. Mater. Chem. **8**, 125 (1998).
5) S. Kimura, T. Iizuka, H. Miyazaki, T. Hajiri, M. Matsunami, T. Mori, A. Irizawa, Y. Muro, J. Kajino, and T. Takabatake, Phys. Rev. B **84**, 165125 (2011).
6) T. Takabatake, F. Iga, T. Yoshino, Y. Echizen, K. Katoh, K. Kobayashi, M. Higa, N. Shimizu, Y. Bando, G. Nakamoto, H. Fujii, K. Izawa, T. Suzuki, T. Fujita, M. Sera, M. Hiroi, K. Maezawa, S. Mock, H. v. Löhneysen, A. Brückl, K. Neumaier, and K. Andres, J. Magn. Magn. Mater. **177-181**, 277 (1998), and references therein.
7) T. Nishioka, Y. Kawamura, T. Takesaka, R. Kobayashi, H. Kato, M. Matsumura, K. Kodama, K. Matsubayashi, and Y. Uwatoko, J. Phys. Soc. Jpn. **78**, 123705 (2009).
8) Y. Muro, J. Kajino, T. Onimaru, and T. Takabatake, J. Phys. Soc. Jpn. **80**, SA021 (2011).
9) S. Kimura, T. Iizuka, H. Miyazaki, A. Irizawa, Y. Muro, and T. Takabatake, Phys. Rev. Lett. **106**, 056404 (2011).
10) S. Kimura, Y. Muro, and T. Takabatake, J. Phys. Soc. Jpn. **80**, 033702 (2011).
11) S. Kimura, H. Tanida, M. Sera, Y. Muro, T. Takabatake, T. Nishioka, M. Matsumura, and R. Kobayashi, Phys. Rev. B **91**, 241120(R) (2015).
12) A. Kondo, K. Kindo, K. Kunimori, H. Nohara, H. Tanida, M. Sera, R. Kobayashi, T. Nishioka, and M. Matsumura, J. Phys. Soc. Jpn. **82**, 054709 (2013).
13) H. Tanida, H. Nohara, M. Sera, T. Nishioka, M. Matsumura, and R. Kobayashi, Phys. Rev. B **90**, 165124 (2014).
14) H. Tanida, H. Nohara, F. Nakagawa, K. Yoshida, M. Sera, and T. Nishioka, Phys. Rev. B **94**, 165137 (2016).
15) R. Kobayashi, Y. Ogane, D. Hirai, T. Nishioka, M. Matsumura, Y. Kawamura, K. Matsubayashi, Y. Uwatoko, H. Tanida, and M. Sera, J. Phys. Soc. Jpn. **82**, 093702 (2013).
16) J. Kawabata, T. Ekino, Y. Yamada, Y. Sakai, A. Sugimoto, Y. Muro, and T. Takabatake, Phys. Rev. B **92**, 201113(R) (2015).
17) J. Kawabata, T. Ekino, Y. Yamada, A. Sugimoto, Y. Muro, and T. Takabatake, Proc. SCES 2016 (2017) in press.
18) J. Kawabata, T. Takabatake, K. Umeo, and Y. Muro, Phys. Rev. B **89**, 094404 (2014).
19) Y. Muro, J. Kajino, K. Umeo, K. Nishimoto, R. Tamura, and T. Takabatake, Phys. Rev. B **81**, 214401 (2010).
20) S. Kimura and H. Okamura, J. Phys. Soc. Jpn. **82**, 021004 (2013).
21) S. Kimura, JASCO Report **50**, 6 (2008). [in Japanese]
22) M. Dressel and G. Grüner, *Electrodynamics of Solids* (Cambridge University Press, Cambridge, UK, 2002).
23) S. Kimura, T. Iizuka, and Y. S. Kwon, J. Phys. Soc. Jpn. **78**, 013710 (2009).
24) S. Kimura, Y. S. Kwon, Y. Matsumoto, H. Aoki, and O, Sakai, J. Phys. Soc. Jpn. **85**, 083702 (2016).
25) T. Iizuka, S. Kimura, A. Herzog, J. Sichelschmidt, C. Krellner, C. Geibel, and F. Steglich, J. Phys. Soc. Jpn. **79**, 123703 (2010).
26) S. Kimura, T. Iizuka, Y. Muro, J. Kajino, and T. Takabatake, J. Phys.: Conf. Ser. **391**, 012030 (2012).
27) F. J. Di Salvo, J. A. Wilson, B. G. Bagley, and J. V. Waszczak, Phys. Rev. B **12**, 2220 (1975).
28) S. Kimura, M. Ikezawa, A. Ochiai, and T. Suzuki, J. Phys. Soc. Jpn. **65**, 3591 (1996).
29) T. Yoshida, T. Ohashi and N. Kawakami, J. Phys. Soc. Jpn. **80**, 064710 (2011).
30) T. Yoshida and N. Kawakami, Phys. Rev. B **85**, 235148 (2012).
31) A. Ochiai, T. Suzuki, and T. Kasuya, J. Phys. Soc. Jpn. **59**, 4129 (1990).
32) V. N. Antonov, A. N. Yaresko, A. Ya. Perlov, P. Thalmeier, and P. Fulde, Phys. Rev. B **58**, 9752 (1998).
33) S. Kimura, T. Nishi, M. Okuno, H. Iwata, H. Aoki, and A. Ochiai, J. Phys. Soc. Jpn. **71**, Suppl. p. 300 (2002).